# microRNA-138 modulates cardiac patterning during embryonic development

Sarah U. Morton[a,b,c,1], Paul J. Scherz[c,d,e,1], Kimberly R. Cordes[a,b,c], Kathryn N. Ivey[a,b,c], Didier Y. R. Stainier[c,d,e], and Deepak Srivastava[a,b,c,2]

[a]Gladstone Institute of Cardiovascular Disease, [b]Departments of Pediatrics, and [c]Biochemistry and Biophysics, [d]Programs in Developmental Biology, Genetics, and Human Genetics, and [e]Cardiovascular Research Institute, University of California, San Francisco, CA 94158

Edited by Eric N. Olson, University of Texas Southwestern Medical Center, Dallas, TX, and approved September 24, 2008 (received for review May 13, 2008)

**Organ patterning during embryonic development requires precise temporal and spatial regulation of protein activity. microRNAs (miRNAs), small noncoding RNAs that typically inhibit protein expression, are broadly important for proper development, but their individual functions during organogenesis are largely unknown. We report that miR-138 is expressed in specific domains in the zebrafish heart and is required to establish appropriate chamber-specific gene expression patterns. Disruption of miR-138 function led to ventricular expansion of gene expression normally restricted to the atrio-ventricular valve region and, ultimately, to disrupted ventricular cardiomyocyte morphology and cardiac function. Temporal-specific knockdown of miR-138 by antagomiRs showed miR-138 function was required during a discrete developmental window, 24–34 h post-fertilization (hpf). miR-138 functioned partially by repressing the retinoic acid synthesis enzyme, aldehyde dehydrogenase-1a2, in the ventricle. This activity was complemented by miR-138-mediated ventricular repression of the gene encoding versican (*cspg2*), which was positively regulated by retinoic-acid signaling. Our findings demonstrate that miR-138 helps establish discrete domains of gene expression during cardiac morphogenesis by targeting multiple members of a common pathway, and also establish the use of antagomiRs in fish for temporal knockdown of miRNA function.**

heart development | organ patterning | retinoic acid | atrioventricular canal | versican

Most organs are composed of cells of similar origin that develop divergent patterns of gene expression and functional properties necessary for myriad biological outcomes. The heart has been a particularly informative model for such organ patterning with numerous transcriptional networks that establish chamber or domain-specific gene expression and function (1). In vertebrates, the linear heart tube forms from the migration and fusion of bilateral cardiac progenitor fields at the midline, followed by cardiac looping to form an s-shaped heart. Distinct atrial and ventricular chambers with unique physiological and electrical properties arise, separated by a discrete domain known as the atrioventricular canal (AVC) (2, 3). The AVC gives rise to the valves that ensure unidirectional flow of blood. In mammals, each chamber and valve-forming region becomes septated, resulting in a four-chambered heart.

Transcriptional networks that establish chamber-specific gene expression are highly conserved across species ranging from zebrafish to humans (1). Zebrafish are particularly informative for studying these early patterning networks because of their relatively simple two-chambered heart and their ability to develop even in the absence of a functioning heart. Ultimately, the atrial and ventricular chambers express distinct *myosin* genes (4), whereas genes such as *cspg2*, encoding versican, and *notch1b* are restricted to the AVC (5).

In addition to transcriptional control of gene expression, post-transcriptional regulation through small noncoding RNAs is emerging as a frequently used cellular mechanism to titrate activity of key regulatory pathways. The class of small, highly conserved noncoding RNAs known as microRNAs (miRNAs) function to fine-tune gene expression during development and, in some cases, can function as major switches of gene programs (6). miRNA precursors, known as primary miRNA (pri-miRNA) are transcribed by RNA polymerase II and processed into approximately 70-nucleotide (nt) hairpins by an enzyme complex containing Drosha (7). These pre-miRNA forms are exported from the nucleus by Exportin5 and cleaved by Dicer to make biologically active 20–25-nt mature miRNAs (8, 9). Sequence-specific interaction of the mature miRNA with mRNA targets, typically involving the 5′ end of the miRNA known as a "seed sequence," can result in translational repression or mRNA degradation (7, 9, 10).

We and others reported that miR-1 regulates gene expression and muscle differentiation during mouse and fly cardiogenesis (11–16); however, evidence for individual miRNAs in patterning distinct domains of the heart or other organs has been lacking (17–21). Here, we show that the highly conserved miRNA, miR-138, helps establish discrete domains of gene expression required for normal cardiac morphogenesis and does so by directly repressing multiple members of a common pathway involving retinoic acid synthesis. In addition, we demonstrate the utility of antagomiR technology in zebrafish to delineate developmental windows of miRNA function.

## Results

**miR-138 Is Expressed in the Zebrafish Heart and Is Required for Normal Cardiogenesis.** We used zebrafish as a model to investigate the regulation of chamber-specific gene expression and cardiac patterning by miRNAs (22). In situ hybridization studies in zebrafish showed restricted cardiac expression of any miRNAs, including miR-138 (23), which was found at high levels in the brain, spinal cord, and outflow tract of the heart at 96 h post fertilization (hpf) and is 100% conserved from fugu to humans [see Supporting Information (SI) Fig. S1*A*]. Further in situ hybridization analysis suggested that cardiac expression of miR-138 was localized to the ventricular chamber at 48 hpf (Fig. 1*A*). To determine whether miR-138 is restricted to cardiac muscle or is also expressed in endothelial and endocardial cells, we isolated these two cell types from transgenic fish at 48 hpf expressing green fluorescent protein (GFP) driven by either the myocardial- or endothelial-specific enhancers of *cmlc2* or *flk1*, respec-

Author contributions: S.U.M., P.J.S., K.R.C., K.N.I., D.Y.R.S., and D.S. designed research; S.U.M. and P.J.S. performed research; S.U.M., P.J.S., K.R.C., K.N.I., D.Y.R.S., and D.S. analyzed data; and S.U.M., P.J.S., K.N.I., and D.S. wrote the paper.

The authors declare no conflict of interest.

This article is a PNAS Direct Submission.

Freely available online through the PNAS open access option.

[1]S.U.M. and P.J.S. contributed equally to this work.

[2]To whom correspondence should be addressed at: 1650 Owens Street, San Francisco, CA 94158. E-mail: dsrivastava@gladstone.ucsf.edu.

This article contains supporting information online at www.pnas.org/cgi/content/full/0804673105/DCSupplemental.

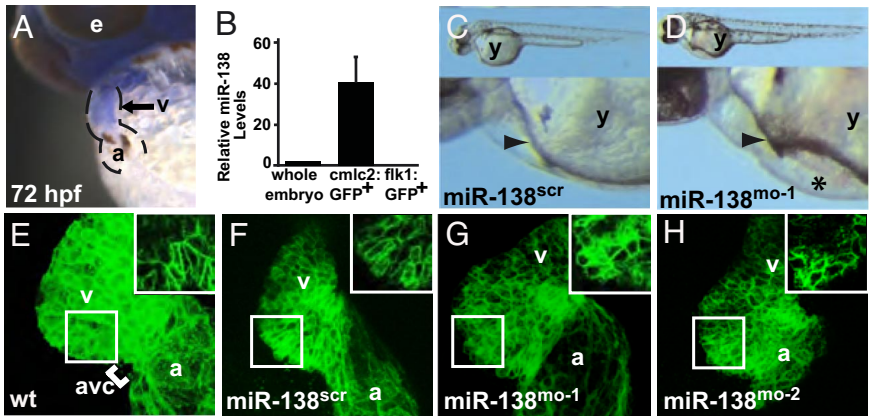


**Fig. 1.** miR-138 is required for cardiac development. (*A*) Oblique view of 72 hpf fish after in situ hybridization showing expression of miR-138 in the ventricular chamber marked by blue staining. (*B*) qRT-PCR analysis of mature miR-138 expression at 48 hpf in flow-sorted cardiomyocytes (cmlc2:GFP), endothelial cells (flk1:GFP), or whole embryos demonstrated enrichment of miR-138 in cardiomyocytes. Mature miR-138 was not detected in endothelial cells. (*C* and *D*) Fish embryos injected with miR-138 scrambled control morpholino (scr) (*C*) or miR-138 morpholino (mo-1) (*D*) showing pericardial edema (asterisk); arrowhead indicates heart. (*E–I*) Representative confocal images of transgenic *Tg(myl7:HRAS-mEGFP)*$^{s843}$ uninjected embryos (*E*) or embryos injected with 17-nt miR-138$^{scr}$ (*F*), 17-nt miR-138$^{mo-1}$ (*G*), or a second 31-nt miR-138$^{mo-2}$ oligo (*H*). Insets show single *z*-stack images of outer curvature ventricular myocytes, which normally elongate with maturation (*E* and *F*) but remained rounded in the miR-138$^{mo}$ embryos (*G* and *H*). (e, eye; y, yolk sac; a, atrium; v, ventricle; avc, atrioventricular canal.)

tively. Mature miR-138 was enriched in cardiomyocytes, but was not detected in the *flk1*-GFP$^{+}$ population (Fig. 1*B*). qRT-PCR for the endothelial-specific gene *egfl7* confirmed that the *flk1*-GFP$^{+}$ population was properly isolated (Fig. S1*B*).

We injected 2–4 ng of a 17-nt morpholino complementary to the mature miR-138 sequence into 1–2-cell embryos to investigate the requirement for miR-138 during cardiac development. At 36 hpf, cardiac function of fish injected with miR-138-specific morpholino (miR-138$^{mo-1}$) was indistinguishable from controls (Movie S1 and Movie S2). At 48 hpf, blood circulation appeared unaffected in the miR-138$^{mo-1}$ fish, but pericardial edema, reflecting cardiac dysfunction, and abnormal looping between the atrial and ventricular chambers were obvious in 60–80% of embryos (Fig. 1 *C* and *D*; Movie S3 and Movie S4). No other gross morphological defects were present in the embryo. Control embryos injected with a 17-nt morpholino scrambled in the region complementary to the 2–7-nt "seed region" of the miRNA (miR-138$^{scr}$) were unaffected. miR-138$^{mo-1}$ fish survived to 72–96 hpf. Blood vessel formation at 24–48 hpf, visualized by using the *Tg(flk1:EGFP)*$^{s843}$ line, which expresses GFP in endothelial cells (3), was unaffected by morpholino injection (Fig. S2).

**miR-138 Is Required for Cardiac Maturation and Patterning in Zebrafish.** Ventricular cardiomyocytes normally become elongated by 48 hpf as they differentiate, whereas myocytes that normally persist around the AVC remain in a more rounded, immature state (24). Confocal microscopy of miR-138$^{mo-1}$ fish revealed defects in elongation of ventricular cardiomyocytes and in cardiac looping at 48 hpf (Fig. 1 *E–H*). About 60% of embryos analyzed by confocal microscopy had myocardial cells along the outer curvature of the ventricle that failed to elongate and remained in a primitive, rounded state typical of less differentiated myocytes ($n$ = 45; Fig. 1 *E–G*). Blood flow and contractility, which are important stimuli for cardiomyocyte maturation (24), appeared grossly intact at 48 hpf (Movie S3 and Movie S4). A second 31-nt morpholino against the pri-miR-138 (mo-2) produced a similar defect, suggesting that the morpholino-induced effects were specifically because of the down-regulation of miR-138 (Fig. 1*H*).

To determine whether cardiac patterning was affected by loss of miR-138, we performed *in situ* hybridization to assess chamber-specific gene expression. At 24 hpf, cardiac myosin light chain 2 (*cmlc2*) mRNA expression, which marks all cardiomyocytes (4), was similar in wild-type and miR-138$^{mo-1}$ fish (Fig. S3 *A* and *B*). The atrial- and ventricular-specific myosin heavy chain (mhc) markers, *amhc* and *vmhc*, respectively, were expressed in appropriate domains at 48 hpf, suggesting normal gross chamber-specification and initial differentiation (Fig. 2 *A–D*) (4, 25).

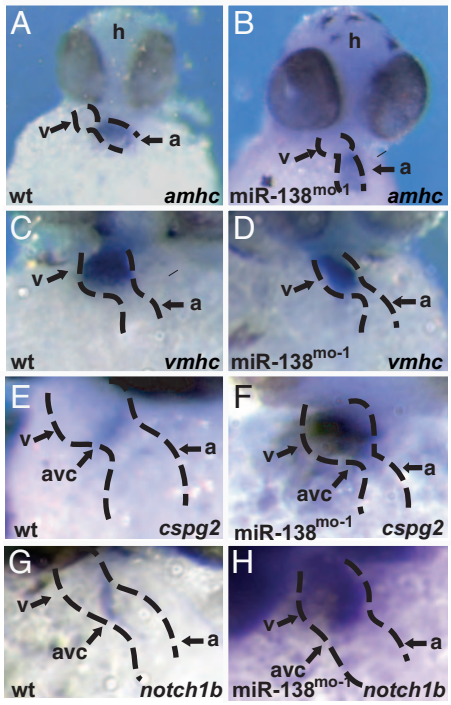


**Fig. 2.** miR-138 knockdown leads to expansion of AVC-specific gene expression into the ventricle. (*A–H*) Ventral views of 48-hpf embryos after mRNA in situ hybridization focusing on head (h) and heart (dotted lines) regions. Atrial (*A* and *B*) and ventricular (*C* and *D*) markers were similar in wild-type (wt) (*A* and *C*) and miR-138$^{mo-1}$ embryos (*B* and *D*). Expression of AVC-specific markers *cspg2* (*E* and *F*) and *notch1b* (*G* and *H*) expanded into the ventricles (v) in miR-138$^{mo-1}$ embryos (*F* and *H*) but not in wild-type embryos (*E* and *G*). (a, atrium; amhc, atrial myosin heavy chain; vmhc, ventricular myosin heavy chain.)

DEVELOPMENTAL BIOLOGY

However, genes normally restricted to the AVC region, including *cspg2* and *notch1b* (5), were ectopically expressed in the ventricle of embryos injected with miR-138$^{mo\text{-}1}$ (Fig. 2 *E–H*) but not in those injected with miR-138$^{scr}$ (Fig. S3 *C–F*). Expanded *cspg2* and *notch1b* expression was also observed in fish treated with the 31-nt morpholino (*cspg2*, 32/41; *notch1b*, 29/35). Versican, the protein encoded by *cspg2*, and Notch1 are involved in valvulogenesis in various animal models (1). Persistence of *cspg2* and *notch1b* transcripts in the ventricle of miR-138$^{mo\text{-}1}$ zebrafish suggests that miR-138 normally restricts the valve-forming domain by repressing AVC gene expression in the ventricle.

**miR-138 Is Required During a Distinct Temporal Window of Cardiac Development.** Cholesterol-conjugated antisense oligonucleotides called antagomiRs can be used to inhibit miRNAs in cell culture and mice, where they broadly diffuse into most cells (26). We tested whether antagomiRs decrease miRNA activity in fish simply on their addition to the water, offering an opportunity to dissect temporal miRNA function in fish. As a proof of concept, we tested antagomiRs targeting miR-451, a miRNA reported to regulate red blood cell maturation in fish by using conventional miR-451 morpholino knockdown methods (27). Addition of miR-451 antagomiR (miR-451$^{am}$) to the water of transgenic fish, containing the red blood cell-specific *gata1* enhancer upstream of red fluorescent protein (RFP), resulted in an absence of RFP$^{+}$ red blood cells, recapitulating the reported effects of miR-451$^{mo}$ (27) (Fig. S4 *A* and *B*). Endothelial cells of the vasculature were intact as marked by *flk1*:EGFP. These findings validated the use of antagomiRs in fish water to knock down miRNA function.

To determine the developmental window during which miR-138 is required, zebrafish were treated with miR-138 antagomiR (miR-138$^{am}$) at various times and collected at 72 hpf. The addition of 2–20 $\mu$M of miR-138$^{am}$ from 24, 30, or 34 hpf decreased mature miR-138 to levels observed on injection of the 31-nt morpholino against pri-miR-138 (Fig. 3*A*). Decreased levels of mature miR-138 were observed up to 5 days after treatment at 24 hpf (Fig. S4*C*). Scrambled antagomiR did not affect miR-138 levels. Exposure of fish to miR-138$^{am}$ between 24 and 72 hpf resulted in defects similar to those observed after miR-138$^{mo\text{-}1}$ injection, including pericardial edema and altered myocardial cell shape (83% vs. 13% with PBS alone, $n = 106$) (Fig. 3 *B–E*). Scrambled antagomiR had effects similar to those of PBS alone. After 30 hpf, 46% ($n = 88$) of treated fish showed cardiac defects, compared with 9% of embryos treated with a scrambled antagomiR or 10% of PBS-treated embryos. By 34 hpf ($n = 88$), embryos were no longer susceptible to miR-138$^{am}$, although the knockdown was still effective. Treatment from 24 hpf also resulted in expansion of *cspg2* mRNA expression into the ventricle, as in miR-138$^{mo\text{-}1}$ embryos (Fig. 3 *F* and *G*). Thus, miR-138 was required between 24 and 34 hpf, which corresponds to the time of early cardiac looping in the fish, but was dispensable thereafter.

**miR-138 Targets *aldh1a2* and *cspg2* in the Developing Zebrafish Heart.** Complimentarity between a miRNA and its target mRNAs, as well as accessibility of the binding site within the 3′UTR of the mRNA, are both important factors in predicting miRNA targets (11, 12, 28). We used a bioinformatics approach incorporating these and other parameters (K.N.I., Y. Zhao, and D.S., unpublished work) to predict mRNA targets of miR-138, and tested 8 potential targets. One, *aldh1a2*, encoding retinoic acid (RA) dehydrogenase (Raldh2), had a highly conserved miR-138 binding site (Fig. 4*A*). Raldh2 is involved in RA synthesis, which is required for early chamber specification and anterior-posterior cardiac patterning in mouse, chick, and zebrafish, and is important for myocardial maturation (29, 30). To test whether miR-138 post-transcriptionally represses *aldh1a2* by directly targeting the 3′UTR, we cloned the zebrafish *aldh1a2* 3′UTR sequence containing the putative miR-138 binding site downstream of a luciferase reporter. The 3′UTR sequence inhibited luciferase activity in response to miR-138, but not miR-1, for which there was not a predicted binding site (Fig. 4*A*, data not shown). Point mutations in the miR-138 binding site, located where nucleotides 2–7 of the miRNA are predicted to bind, abolished repression, indicating that miR-138 can directly target this binding site in the 3′UTR of *aldh1a2*.

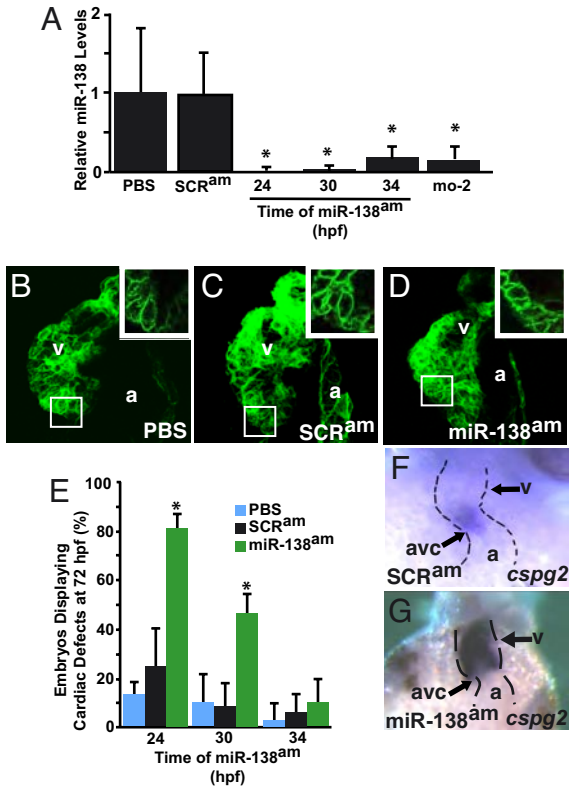


**Fig. 3.** Temporal regulation of miRNA function by antagomiRs in zebrafish. (*A*) miR-138 RNA levels detected by qRT-PCR in 72-hpf fish embryos treated with antagomiRs from 24, 30, or 34 h postfertilization (hpf) or injected with the 31-nt morpholino (mo-2) compared with PBS- or scrambled antagomiR-treated controls. (*B–D*) Confocal images of hearts of 72-hpf *Tg(myl7:HRAS-mEGFP)*$^{s843}$ transgenic embryos treated with PBS (*B*), scrambled antagomiR (SCR$^{am}$) (*C*), or miR-138 antagomiR (miR-138$^{am}$) (*D*) from 24–72 hpf. GFP revealed rounded myocyte morphology (*Inset*) in miR-138$^{am}$ embryos compared to the normally elongated myocytes seen in controls. (*E*) Pericardial edema indicating cardiac dysfunction and rounded ventricular myocytes reflecting delayed maturation were observed in varying percentages of 72-hpf embryos treated with PBS, SCR$^{am}$, or miR-138$^{am}$ from the hpf indicated. (*F* and *G*) Ventral view of mRNA in situ hybridization to detect *cspg2* expression in hearts of embryos treated with SCR$^{am}$ (*F*) or miR-138$^{am}$ (*G*) showed expansion of *cspg2* into the ventricle of miR-138$^{am}$ embryos; heart is indicated with dotted lines. Results shown are the average of four experiments in (*A*) and (*E*). (v, ventricle; a, atrium; atrioventricular canal (avc); *, $P < 0.05$.)

Injection of pri-miR-138 into fish decreased, and exposure to miR-138 antagomiR increased, endogenous *aldh1a2* mRNA levels, demonstrating regulation of *aldh1a2* by miR-138 *in vivo* (Fig. 4*B*). In wild-type hearts, Raldh2 protein was enriched in the AVC region, but hardly detectable in the remaining heart tube (Fig. 4*C*). In contrast, Raldh2 protein expression was expanded into the ventricle of miR-138$^{am}$ embryos, and the area of cardiac Raldh2 immunostaining was increased fivefold, consistent with it being a direct target normally repressed in the ventricle (Fig. 4*D* and Fig. S5*A*). AntagomiR treatment of embryos transgenically expressing GFP in endothelial cells or cardiomyocytes revealed that Raldh2 protein was present in endothelial cells in

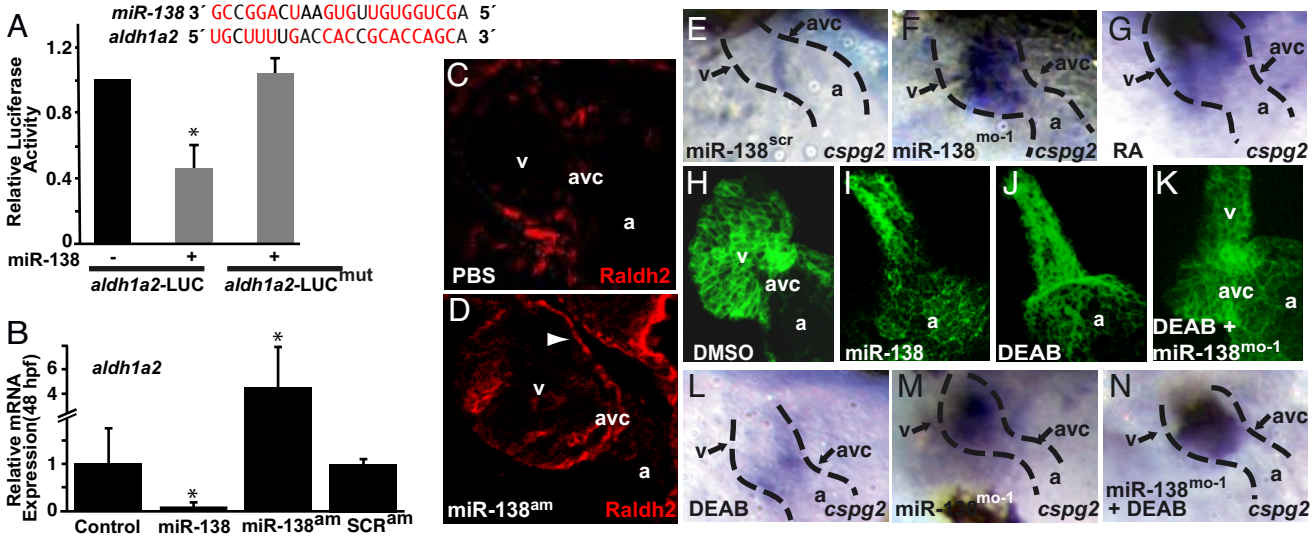


**Fig. 4.** miR-138 directly targets *aldh1a2*, restricting its expression to the AVC. (*A*) miR-138 binding site in zebrafish *aldh1a2* 3′ UTR with complementary nucleotides indicated in red. Luciferase activity in Cos cells on introduction of wild-type or mutated (mut) *aldh1a2* 3′ UTR sequences downstream of a CMV-driven luciferase reporter with or without miR-138 is shown. (*B*) *aldh1a2* mRNA levels measured by qRT-PCR in embryos injected with pri-miR-138 or treated at 24 hpf with miR-138 antagomiR (miR-138$^{am}$) or scrambled antagomiR (SCR$^{am}$). Results shown represent at least 4 experiments in (*A*) and (*B*). Error bars indicate 95% confidence intervals. (*C* and *D*) Raldh2 immunohistochemistry on sections of 72-hpf embryos treated with PBS or miR-138$^{am}$ from 24–72 hpf. Ventricular (v) cardiomyocyte expression (arrowhead) was readily detectable in miR-138$^{am}$ hearts but not in controls, whereas intensity of staining in the AVC was similar. (*E–G*) Ventral view of *cspg2* expression in the heart by mRNA in situ hybridization in embryos treated with scrambled morpholino (miR-138$^{scr}$) (*E*), miR-138$^{mo-1}$ (*F*), or retinoic acid (RA) (*G*); heart is indicated with dotted lines. (*H–K*) Confocal images of *myl7-GFP* embryos (48 hpf) treated with vehicle (DMSO) (*H*), premiR-138 RNA (*I*), or DEAB (*J*), and DEAB-treated embryos also injected with miR-138$^{mo-1}$ (*K*) showing rescue of the linear heart tube phenotype with knockdown of miR-138. (*L–N*) Expansion of *cspg2* mRNA expression from the avc (*L*) into the ventricle (v) of miR-138$^{mo-1}$ embryos (*M*) was not rescued by DEAB (*N*). (a, atrium; ∗, $P < 0.05$.)

the AVC, but was aberrantly expressed in cardiomyocytes in the ventricle (Fig. S5 *B* and *C*). In situ hybridization analysis of Raldh2 mRNA also revealed expansion of the mRNA expression in the ventricle of miR-138$^{mo}$ embryos but not in controls (Fig. S5 *D* and *E*).

Although it is likely that many miR-138 targets mediate its effects on cardiac patterning and gene expression, we sought to determine to what degree RA signaling may contribute to the miR-138 knockdown phenotype. Exogenous RA administered 24–48 hpf caused expansion of *cspg2* expression into the ventricle, similar to that observed in miR-138$^{mo}$ embryos (Fig. 4 *E–G*), consistent with increased RA signaling in the ventricle contributing to ventricular *cspg2* transcription. Conversely, inhibiting RA signaling with 4-(diethylamino)benzaldehyde (DEAB) (31) between 24–48 hpf in wild-type embryos produced a linear heart, similar to the phenotype of miR-138 overexpression, in which RA signaling was reduced (Fig. 4 *H–J*). The DEAB knockdown phenotype was significantly rescued by knockdown of miR-138, providing further evidence of miR-138 regulation of RA signaling (Fig. 4*K*).

Curiously, inhibition of RA signaling in miR-138$^{mo}$ embryos did not rescue aberrant ventricular expression of *cspg2* or *notch1b* (Fig. 4 *L–N* and data not shown), indicating that they were affected by miR-138 independently of altered RA signaling, and raising the possibility they may also be direct targets of miR-138. The *notch1b* 3′UTR did not contain any miR-138 binding sites and was not responsive to miR-138, suggesting transcriptional regulation (Fig. S6). Because the 3′-UTR of zebrafish *cspg2* has not been annotated, we examined the mouse *cspg2* 3′UTR, given the 100% conservation of zebrafish and mouse miR-138. As in *aldh1a2*, we found a miR-138 binding site in the *cspg2* 3′UTR that was responsive to miR-138 (Fig. 5*A*). Introduction of miR-138 into mouse NIH 3T3 cells decreased endogenous *cspg2* mRNA and protein accumulation by approximately 40% (Fig. 5 *B* and *C*). Furthermore, miR-138 RNA injection into zebrafish embryos decreased endogenous *cspg2* mRNA levels by 90% (Fig. 5*D*). Treatment with miR-138 antagomiR increased endogenous *cspg2* mRNA levels eightfold, whereas scrambled antagomiR had no effect. Thus, miR-138 not only restricts versican expression to the AVC region by regulating retinoic acid synthesis, but may also directly repress *cspg2* in the ventricle posttranscriptionally in addition to its effects on *cspg2* transcriptional regulation.

## Discussion

We have found that miR-138 represses AVC-specific transcripts in the developing ventricle by regulating a network of developmental signals. This ultimately contributes to ventricular cardiomyocyte maturation and thereby helps to establish the distinct identity of cardiac structures. Specifically, miR-138 represses RA signaling in the ventricles and reinforces its influence on this pathway by negatively regulating *cspg2*, which is downstream of RA and is AVC specific (Fig. 5*E*). Other yet unknown genes regulated by miR-138 may also be involved in this process. Our findings provide an example of how miRNA-based networks can refine discrete patterns of gene expression during organogenesis to control the formation of functionally distinct domains. In this case, miR-138's function to "clear" unwanted mRNA expression from a specific region of the heart is similar to miR-430's role in clearing residual maternal mRNAs from the developing zebrafish embryo (18).

The rescue of the DEAB phenotype by miR-138 knockdown suggests that cardiac patterning is co-regulated by miR-138 and RA. During migration of the bilateral heart fields early in development, an anterior-posterior gradient of RA signaling generated by the posterior mesoderm drives cardiac progenitors to an atrial fate (29). Raldh2, which converts retinaldehyde to retinoic acid, is expressed early in mouse development and its targeted deletion results in cardiac defects by embryonic day 9.5, including a lack of looping and a single chamber morphology (32). The looping defect in *Raldh2* mouse mutants can be rescued by exogenous treatment of retinoic acid. In addition to

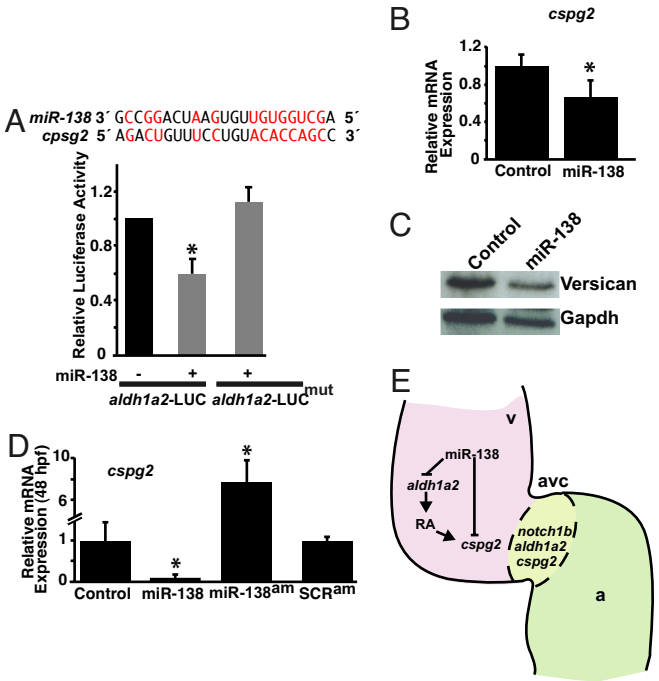


**Fig. 5.** miR-138 directly targets *cspg2*. (*A*) Sequence of miR-138 and its binding site in mouse *cspg2* 3′ UTR with complementary nucleotides indicated in red. Luciferase activity in Cos cells on introduction of wild type or mutated (mut) *cspg2* 3′ UTR sequences downstream of a CMV-driven luciferase (LUC) reporter with or without miR-138 is shown. (*B* and *C*) Analysis of *cspg2* mRNA level assessed by qRT-PCR (*B*) and corresponding versican protein by western blot (*C*) in mouse NIH 3T3 fibroblasts transfected with miR-138. (*D*) *cspg2* mRNA levels detected by qRT-PCR in zebrafish embryos injected with miR-138 or treated at 24 hpf with miR-138 antagomiR (am) or scrambled (SCR) antagomiR. (*E*) Proposed model for the function of miR-138 in regulating chamber-specific gene expression and atrioventricular canal (avc) patterning. miR-138 directly represses retinoic acid (RA) synthesis in the ventricle (v) via *aldh1a2*, which would otherwise induce expression of the avc-specific gene, *cspg2* (versican). Repression of *cspg2* by miR-138 in the ventricle is also accomplished by directly targeting *cspg2*. Results shown in (*A*), (*B*), and (*D*) represent at least 4 experiments with error bars indicating 95% confidence intervals. (a, atrium; *, $P < 0.05$.)

these known roles of RA signaling in early cardiac patterning, we have shown that restricted AVC expression of Raldh2 at 48 hpf is also necessary for proper ventricular development. Ectopic ventricular Raldh2 in miR-138$^{mo}$ embryos may contribute to the mispatterning of the AVC and ventricle by altering the amount and distribution of RA.

In contrast, the observed defects in myocardial maturation, which were not rescued by DEAB, may be influenced by increased expression of versican and other targets that have not yet been identified. miR-138 affected *cspg2* expression through RA signaling and by targeting it directly, thereby repressing AVC gene expression in the ventricle by multiple avenues. However, the degree to which *cspg2* or *notch1b* up-regulation contributes to the cardiomyocyte maturation defect in miR-138$^{mo}$ embryos remains unknown, as knockdown of *cspg2* yielded early gastrulation defects, precluding such studies. Knockdown of miRNA targets at later developmental time points, as will become possible with caged morpholinos and other evolving technologies, could allow further dissection of each target's contribution to the miR-138 knockdown phenotype.

Finally, our finding that antagomiRs can regulate zebrafish miRNA function simply by addition to the environment will allow temporal resolution of miRNA function. Current methods (33) cannot determine temporally specific roles of miRNAs, which is particularly important when studying genes required for early development that may also have later physiologic functions. Use of antagomiRs in this model system bypasses these hurdles. Future studies of miRNAs in zebrafish will benefit from this temporal resolution. It will be interesting to determine whether this method is also applicable to mRNA knockdown.

## Materials and Methods

**Zebrafish Lines.** Wild-type *AB* and transgenic *Tg(myl7:HRAS-mEGFP)$^{s843}$* (Myl7-GFP), *Tg(flk1:EGFP)$^{s843}$* (flk1-GFP), and *Tg(flk1:EGFP, gata1:RFP)$^{s843}$* zebrafish (34) were raised under standard laboratory conditions at 28 °C (35).

**Microinjection.** A 350 nt pri-miR-138 fragment was cloned from mouse cDNA and ligated into the pCR-II vector. RNA was made by in vitro transcription with the SP6 promoter. Embryos were injected at the 1–2-cell stage with 2–5 ng of miR-138 MO [5′-GAUUCACAACACCAGCU-3′, Integrated DNA Technologies (IDT)], 2–5 ng of scrambled MO (5′-GAUUGGAAACACCAGCU-3′, IDT), 2–5 ng pri-miR-138 MO (5′-GTGACATCGGCCTGATTCACAACACCAGCTG-3′, GeneTools), or 100–200 pg *pri-miR-138–2* RNA. The embryos were maintained at 28 °C until harvesting.

**Confocal Analysis.** Embryos were fixed in 2% paraformaldehyde (PFA) overnight, embedded in 4% low-melt agarose, and cut into 150-$\mu$m sections with a Leica VT1000S vibratome. Images were acquired with a Zeiss LSM5 Pascal confocal microscope.

**AntagomiR Treatment.** All zebrafish embryos were manually dechorionated and treated with 2–20 $\mu$M antagomiR. AntagomiR targeting miR-451 (Dharmacon) was added at 12–24 hpf, and embryos were examined at 32–60 hpf. AntagomiR miR-138 (5′-GAUUCACAACACCAGCU-3′, IDT), scrambled antagomiR (5′-GAUUGGAAACACCAGCU-3′, IDT), or PBS was added to water at 24, 30, or 34 hpf and visualized at 72 hpf. Because of variability between preparations, antagomiRs were assayed for efficacy by injection into 1–2-cell embryos before exogenous use. Phenotype results were averaged from four experiments.

**Immunohistochemistry.** Embryos were fixed for 1 h at room temperature in 4% PFA, incubated in 20% sucrose/PBS overnight, embedded in OCT, and sectioned with a cryostat. Sections were washed in PBS with 0.05% Triton and incubated with rabbit anti-Raldh2 antibody (generous gift of Dr. Peter McCaffery) overnight at a 1:200 dilution. This antibody is specific for Raldh2 protein in zebrafish (36). The embryos were then incubated in secondary antibody [1:200 Alexa Fluor 574 conjugated goat anti-rabbit antibody (Molecular Probes)] overnight and washed. Images were acquired with a Zeiss LSM5 Pascal confocal microscope.

**In Situ Hybridization.** Probes against miR-138 (Exiqon), *cmlc2* (4), *amhc* (25), *vmhc* (4), *cspg2* (5), *notch1b* (5), and *aldh1a2* were used. miR-138 in situ hybridization was performed according to published protocols (Exiqon). Probes against mRNAs were synthesized, and in situ hybridizations were performed as described (37).

**Luciferase Assay.** miRNA target prediction software developed in the Srivastava laboratory was used to bioinformatically identify potential targets of miR-138. 428 nucleotides (1,632–2,058, NM_131850) of *Danio rerio aldh1a2* and 280 nucleotides (10,755–11,032, NM_001081249) of *Mus musculus cspg2* 3′-UTRs predicted to contain miR-138 binding sites were cloned into the pGL3 vector (Promega). Point mutations of the binding sites were generated by using QuikChange II PCR (Stratagene). pri-miR-138–2 was subcloned into the pSilencer-3.1 vector (Ambion). Renilla-encoding vector was used as a transfection control. Cos-1 cells were transfected with 350 ng of miR-138, 150 ng of CMV-luciferase, and 50 ng of CMV-renilla constructs with Fugene (Roche), and cells were harvested after 48 h. Luciferase and renilla activity were assayed with the Dual-Reporter Assay (Promega). Results shown are from triplicate experiments.

**Transient Transfection.** NIH 3T3 mouse fibroblasts were grown in DMEM supplemented with 5% calf serum and penicillin/streptomycin (Gibco). Cells were transfected with 1.5 $\mu$g of GFP, miR-1, or miR-138 constructs with the nucleofection program U-30 (Amaxa). After 20 h, cells were collected directly in Trizol (Invitrogen). Transfection efficiency was above 95%.

**Quantitative Real-Time RT-PCR.** RNA was prepared from whole embryos injected with pre-miR-138–2, the anterior portion of embryos treated with

antagomiRs, or NIH 3T3 mouse fibroblasts with Trizol (Invitrogen). To isolate myocardial and endocardial/endothelial cells, 48-hpf fish were dissected to remove the head and trunk and then digested with 2% trypsin. GFP+ cells were isolated from the resulting single-cell suspension by flow cytometry. For mRNA qRT-PCR, cDNA was reverse transcribed with an oligo(dT) primer. Custom primers for *Danio rerio cspg2*, and *alhla2* and inventoried primers for *Mus musculus cspg2*, *gapdh*, and *aldh1a2* were used for Taqman-based real-time RT-PCR (Applied Biosystems). For miRNA qRT-PCR, cDNA was reverse transcribed from 10 ng of total RNA with the Taqman microRNA Reverse Transcription Kit (Applied Biosystems). miR-26a was used as an endogenous control. Results represent at least three experiments.

**Pharmocological Treatment.** Embryos were dechorionated and treated with retinoic acid (Sigma) at a final concentration of 0.1–1 $\mu$M or DEAB (Sigma) diluted to a final concentration of 25 $\mu$M, both with a final concentration of 0.25% DMSO. The embryos were maintained at 28 °C until harvesting.

**Statistical Analysis.** Results from at least three trials were averaged and the 95% confidence interval calculated and plotted as error bars. Significance was determined by using the unpaired student *t* test.

**ACKNOWLEDGMENTS.** We thank A. Muth, P. Aanstad, C. Shin, and all members of the Srivastava and Stainier labs for assistance, invaluable support, and discussion. L. Prentice (University of California, San Francisco) processed frozen sections for immunohistochemistry. Bioinformatics analysis of zebrafish *cspg2* gene was performed by S. Chatterji and L. Pachter. G. Howard provided editorial assistance, and B. Taylor assisted with graphics and manuscript preparation. Support for this work came from the American Heart Association (AHA) Western Affiliates (S.U.M.), Helen Hay Whitney Foundation (P.J.S), California Institute for Regenerative Medicine (K.N.I.), U.S. National Institutes of Health [HL-54737 (D.Y.R.S.)], and Packard Foundation (D.Y.R.S.). D.S. was supported by grants from the National Heart, Lung, and Blood Institute/National Institutes of Health, AHA, March of Dimes Birth Defects Foundation, and the California Institute of Regenerative Medicine.

1. Srivastava D (2006) Making or breaking the heart: From lineage determination to morphogenesis. *Cell* 126:1037–1048.
2. Stainier DY (2001) Zebrafish genetics and vertebrate heart formation. *Nat Rev Genet* 2:39–48.
3. Beis D, *et al*. (2005) Genetic and cellular analyses of zebrafish atrioventricular cushion and valve development. *Development* 132:4193–4204.
4. Yelon D, Horne SA, Stainier DY (1999) Restricted expression of cardiac myosin genes reveals regulated aspects of heart tube assembly in zebrafish. *Dev Biol* 214:23–37.
5. Walsh EC, Stainier DY (2001) UDP-glucose dehydrogenase required for cardiac valve formation in zebrafish. *Science* 293:1670–1673.
6. Zhao Y, Srivastava D (2007) A developmental view of microRNA function. *Trends Biochem Sci* 32:189–197.
7. Lee Y, *et al*. (2003) The nuclear RNase III Drosha initiates microRNA processing. *Nature* 425:415–419.
8. Yi R, Qin Y, Macara IG, Cullen BR (2003) Exportin-5 mediates the nuclear export of pre-microRNAs and short hairpin RNAs. *Gene Dev* 17:3011–3016.
9. Hutvagner G, *et al*. (2001) A cellular function for the RNA-interference enzyme Dicer in the maturation of the let-7 small temporal RNA. *Science* 293:834–838.
10. Gregory RI, Chendrimada TP, Cooch N, Shiekhattar R (2005) Human RISC couples microRNA biogenesis and posttranscriptional gene silencing. *Cell* 123:631–640.
11. Zhao Y, Samal E, Srivastava D (2005) Serum response factor regulates a muscle-specific mircroRNA that targets *Hand2* during cardiogenesis. *Nature* 436:214–220.
12. Kwon C, Han Z, Olson EN, Srivastava D (2005) MicroRNA1 influences cardiac differentiation in Drosophila and regulates Notch signaling. *Proc Natl Acad Sci USA* 102:18986–18991.
13. Sokol NS, Ambros V (2005) Mesodermally expressed *Drosophila* microRNA-1 is regulated by Twist and is required in muscles during larval growth. *Gene Dev* 19:2343–2354.
14. Zhao Y, *et al*. (2007) Dysregulation of cardiogenesis, cardiac conduction, and cell cycle in mice lacking miRNA-1–2. *Cell* 129:303–317.
15. Chen JF, *et al*. (2006) The role of microRNA-1 and microRNA-133 in skeletal muscle proliferation and differentiation. *Nat Genet* 38:228–233.
16. Ivey KN, *et al*. (2008) MicroRNA regulation of cell lineages in mouse and human embryonic stem cells. *Cell Stem Cell* 2:219–229.
17. Wienholds E, Koudijs MJ, van Eeden FJ, Cuppen E, Plasterk RH (2003) The microRNA-producing enzyme Dicer1 is essential for zebrafish development. *Nat Genet* 35:217–218.
18. Giraldez AJ, *et al*. (2005) MicroRNAs regulate brain morphogenesis in zebrafish. *Science* 308:833–838.
19. Bernstein E, *et al*. (2003) Dicer is essential for mouse development. *Nat Genet* 35:215–217.
20. Harfe BD, McManus MT, Mansfield JH, Hornstein E, Tabin CJ (2005) The RNaseIII enzyme Dicer is required for morphogenesis but not patterning of the vertebrate limb. *Proc Natl Acad Sci USA* 102:10898–10903.
21. Harris KS, Zhang Z, McManus MT, Harfe BD, Sun X (2006) Dicer function is essential for lung epithelium morphogenesis. *Proc Natl Acad Sci USA* 103:2208–2213.
22. Glickman NS, Yelon D (2002) Cardiac development in zebrafish: Coordination of form and function. *Semin Cell Dev Biol* 13:507–513.
23. Wienholds E, *et al*. (2005) MicroRNA expression in zebrafish embryonic development. *Science* 309:310–311.
24. Auman HJ, *et al*. (2007) Functional modulation of cardiac form through regionally confined cell shape changes. *PLoS Biol* 5:e53.
25. Berdougo E, Coleman H, Lee DH, Stainier DY, Yelon D (2003) Mutation of weak atrium/atrial myosin heavy chain disrupts atrial function and influences ventricular morphogenesis in zebrafish. *Development* 130:6121–6129.
26. Krutzfeldt J, *et al*. (2005) Silencing of microRNAs in vivo with 'antagomirs'. *Nature* 438:685–689.
27. Dore LC, *et al*. (2008) A GATA-1-regulated microRNA locus essential for erythropoiesis. *Proc Natl Acad Sci USA* 105:3333–3338.
28. Brennecke J, Stark A, Russell RB, Cohen SM (2005) Principles of microRNA-target recognition. *PLoS Biol* 3:e85.
29. Stainier D, Fishman M (1992) Patterning the zebrafish heart tube: Acquisition of anteroposterior polarity. *Dev Biol* 153:91–101.
30. Xavier-Neto J, Shapiro MD, Houghton L, Rosenthal N (2000) Sequential programs of retinoic acid synthesis in the myocardial and epicardial layers of the developing avian heart. *Dev Biol* 219:129–141.
31. Perz-Edwards A, Hardison NL, Linney E (2001) Retinoic acid-mediated gene expression in transgenic reporter zebrafish. *Dev Biol* 229:89–101.
32. Niederreither K, Subbarayan V, Dolle P, Chambon P (1999) Embryonic retinoic acid synthesis is essential for early mouse post-implantation development. *Nat Genet* 21:444–448.
33. Nasevicius A, Ekker SC (2000) Effective targeted gene 'knockdown' in zebrafish. *Nat Genet* 26:216–220.
34. D'Amico L, Scott IC, Jungblut B, Stainier DY (2007) A mutation in zebrafish hmgcr1b reveals a role for isoprenoids in vertebrate heart-tube formation. *Curr Biol* 17:252–259.
35. Westerfield M (2000) in *The Zebrafish Book. A Guide for the Laboratory Use of Zebrafish* (*Danio rerio*), (University of Oregon Press, Eugene), 4th Ed.
36. Prabhudesai SN, Cameron DA, Stenkamp DL (2005) Targeted effects of retinoic acid signaling upon photoreceptor development in zebrafish. *Dev Biol* 287:157–167.
37. Aanstad P, Whitaker M (1999) Predictability of dorso-ventral asymmetry in the cleavage stage zebrafish embryo: An analysis using lithium sensitivity as a dorso-ventral marker. *Mech Dev* 88:33–41.